# ABC mesogens: a novel 'hexagonal columns-in-lamellae' morphology of low molar mass partially fluorinated 'three-chain' benzoic acids

A. Schaz[a]; G. Lattermann[a]

[a] Makromolekulare Chemie I, Universität Bayreuth, D-95440 Bayreuth, Germany

## PLEASE SCROLL DOWN FOR ARTICLE

Taylor & Francis
Taylor & Francis Group

# ABC mesogens: a novel 'hexagonal columns-in-lamellae' morphology of low molar mass partially fluorinated 'three-chain' benzoic acids

A. SCHAZ and G. LATTERMANN*

Makromolekulare Chemie I, Universität Bayreuth, D-95440 Bayreuth, Germany

Two homologous series of 3,4,5-tris(perfluoroalkylalkyloxy)benzoic acids (**K3S[*n,m*]**), with alkyl chain lengths **_m_**=8 and 11 and perfluoroalkyl chain length **_n_**=6,8 and 10, have been investigated with respect to their liquid crystalline behaviour and, in particular, the structure of the mesophases exhibited. The mesophase characterization was performed by means of polarising optical microscopy, differential scanning calorimetry and X-ray diffraction of powder-like samples. At a first glance, the results for each compound indicate the presence of a classical hexagonal columnar mesophase. However, a comparative study of the small angle diffractograms of the two series with alkyl chain lengths **_m_**=8 and 11 reveal an increasing lamellar arrangement within the hexagonal columnar lattice on increasing the perfluoroalkyl chain length **_n_**. A conclusive explanation leads to a mesophase structure combining both a hexagonal arrangement of the carboxylic groups and a layer arrangement of the perfluoroalkyl chains. The model has been proved by simulation of the X-ray diffractograms using corresponding molecular models. This is the first evidence for the existence of a 'hexagonal columns-in-lamellae' morphology, realized by low molar mass compounds, and is analogous to a similar phase structure of linear ABC triblock copolymers.

## 1. Introduction

Microsegregation is regarded to be one of the driving forces for the formation of liquid crystalline phases with, for example, smectic, columnar or cubic morphologies. The space filling of the amphiphilic structural units (linear, wedge or cone-shaped, respectively) determines the type of mesophase obtained. In conventional amphiphilic liquid crystals with polar and apolar parts, the resulting morphologies have close similarities to the phases exhibited by AB diblock copolymers. The segregation of block copolymers is caused to a large extent by the low mixing entropy of the different polymer segments [1], whereas the different molecular moieties of an amphiphilic mesogen segregate because of a sufficiently strong incompatibility, due to a large positive mixing enthalpy.

For example, the AB block copolymer poly(styrene-*block*-polyisoprene) forms different phases, depending on the degree of polymerization of each block. The dependence of the resulting phases, on the volume fraction $\varphi_B$ of the B-block, is shown in figure 1 (*a*). For

low molar mass materials, the glucitol benzoate system, cf. figure 1 (*b*), is a good example of a liquid crystalline material exhibiting comparable structures [2, 3]. In both cases, increasing one part, i.e. extending one chain of the block copolymer or increasing one segment of the low molar mass amphiphilic mesogen, causes a change from (i) a lamellar structure (equal amounts of A and B) to (ii) one of the bicontinous cubic phases (nomenclature for block copolymers: e.g. gyroid; for mesogens: $Cub_{bi}$), then (iii) the hexagonal columnar phase (nomenclature for block copolymers: cylindrical, HEX; for mesogens: $Col_h$) and finally (iv) to one of the spheroidic cubic phases (nomenclature for block copolymers: spherical, e.g. BCC; for mesogens: $Cub_s$). This corresponds to an increasing interfacial curvature.

For several years, linear and star-like ABC triblock copolymers, consisting of three different, incompatible polymer blocks have also been investigated. With respect to the diblock copolymers, the additional third block leads to a strongly increased variety of possible morphologies. The structures are mainly dependent on the degree of incompatibility and the degree of polymerization [4–8]. A selection of some typical phases of linear ABC triblock copolymers is presented in figure 2 [5, 7].

*Corresponding author.
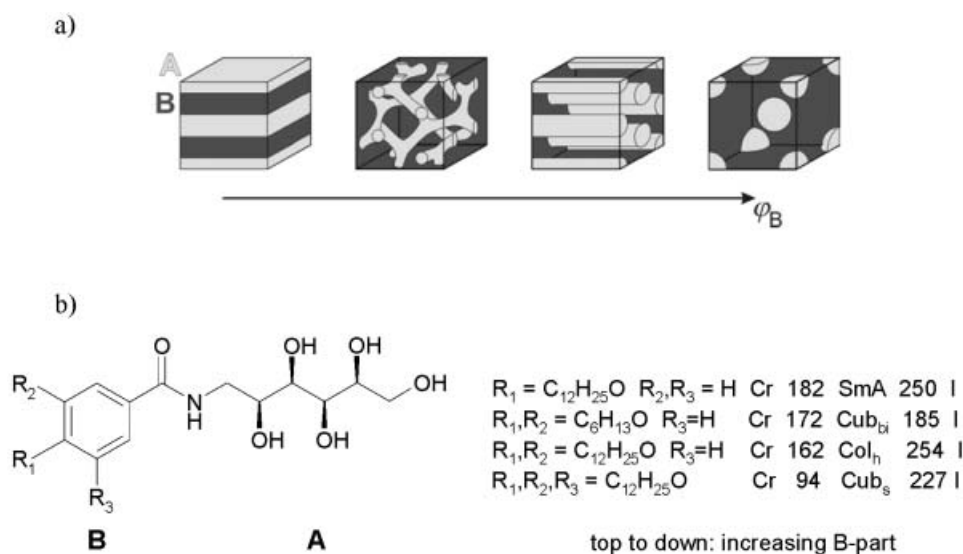Email: guenter.lattermann@uni-bayreuth.de

*A. Schaz and G. Lattermann*

Figure 1.   (*a*) Phase sequence of an AB block copolymer system; e.g. poly(styrene-*block*-polyisoprene). $\varphi_B$ is the volume fraction of block B. (*b*) Phase sequence of a low molar mass AB LC system.
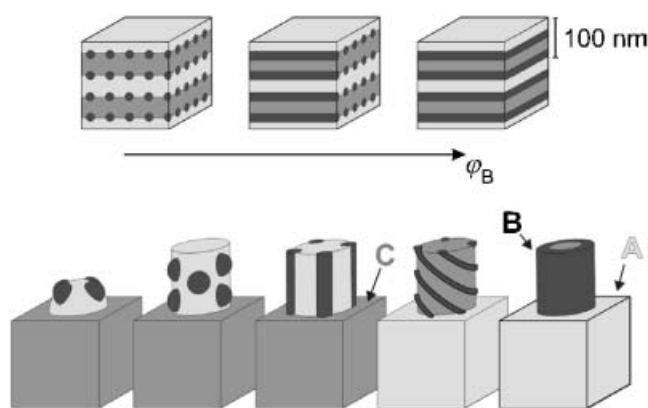


Figure 2.   Examples of morphologies of linear ABC triblock copolymers [5, 7]. $\varphi_B$ is the volume fraction of block B.

The question arises, whether it is possible also to create comparable structures with low molar mass liquid crystalline compounds (ABC mesogens). Hence, the entropic segregation in the polymer system has to be replaced by an enthalpic one. This would require highly incompatible units in the same molecule, e.g. hydrophilic groups (polar groups), hydrophobic groups (e.g. alkyl chains) and lipophobic groups (e.g. perfluoroalkyl segments with their strong tendency to segregate from other organic moieties [9–13 and references therein]).

In a preceding paper [14], we presented the mesomorphic behaviour of succinimidyl benzoates, substituted with one, two and three perfluoroalkyl alkoxy chains ('one-', 'two-' and 'three-chain' compounds **K1NS**, **K2NS** and **K3NS**, respectively). Although built

up from three incompatible moieties, we obtained no direct evidence for a special, new mesophase. With one-chain derivatives, these compounds exhibit smectic phases; with two- and three-chain compounds hexagonal columnar phases are seen. In a further paper [15], dealing with the corresponding one- and two-chain acids **K1S** and **K2S**, we showed that, with respect to the corresponding succinimidyl esters **K*x*NS** even their higher intramolecular polarity contrast does not lead to any evidence for a new mesophase with respect to the molecular ABC structure. Nevertheless, all the phases of these partially fluorinated compounds were assumed to exhibit a clear sequence of their ABC segments, as shown schematically in figure 3 for the succinimidyl esters **K*x*NS** in their smectic or columnar arrangements.

In this paper, we present the mesomorphic properties of the partially fluorinated three-chain acids **K3S** and discuss their ability to form a new mesophase.

## 2.   Results and discussion

The synthesis of the 3,4,5-tris(perfluoroalkylalkyloxy) benzoic three-chain acids **K3S** has been reported in detail in an earlier paper [14], their structure is shown in figure 4. The abbreviation of the compound name results from the number of chains (**K3**), the type of the compound (**S** for acid) and the chain length **[*n,m*]** (***n*** for the perfluoroalkyl and ***m*** for the alkyl chain).

Several partially fluorinated three-chain acids **K3S** were already reported in the literature to exhibit hexagonal columnar phases [10–12]. The new compounds have been investigated by polarising optical microscopy (POM), differential scanning calorimetry
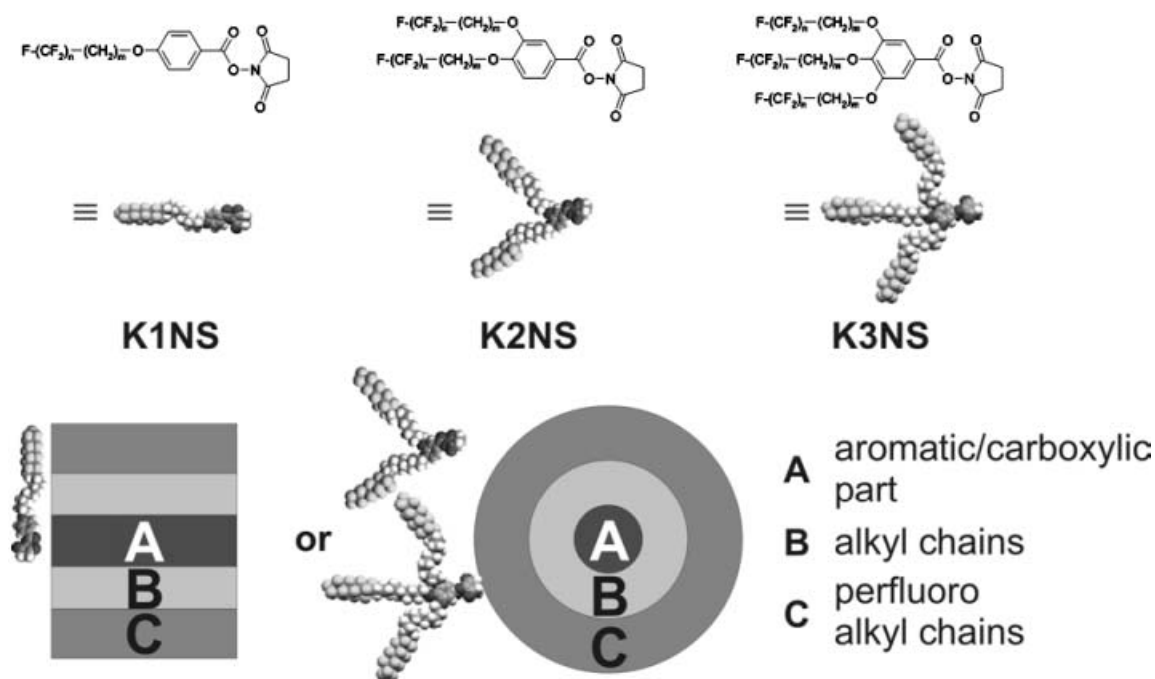
Figure 3.    Schematic models of ABC morphologies of 'one-', 'two-' and 'three-chain' succinimidyl esters **K*x*NS**.
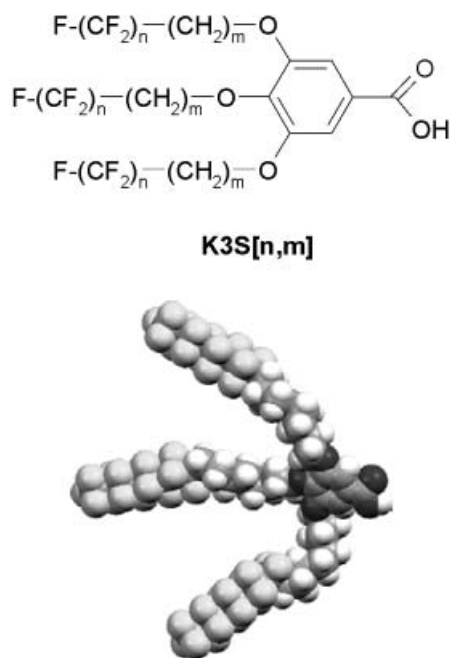


**K3S[n,m]**



Figure 4.    Structure of the investigated three-chain acids **K3S**.

(DSC) and X-ray diffraction (XRD) of non-oriented samples. The thermal data are collected in table 1, together with data taken from the literature. The three-dimensional ba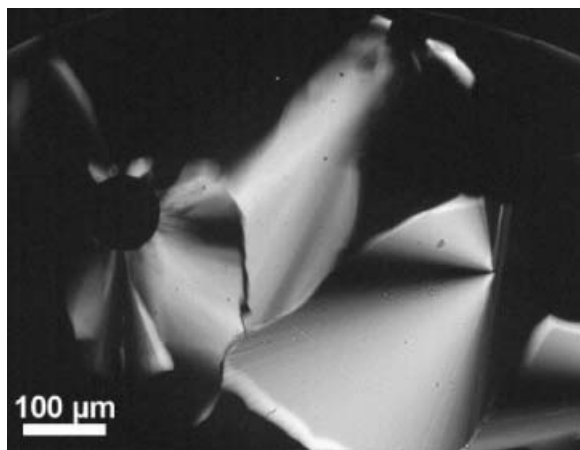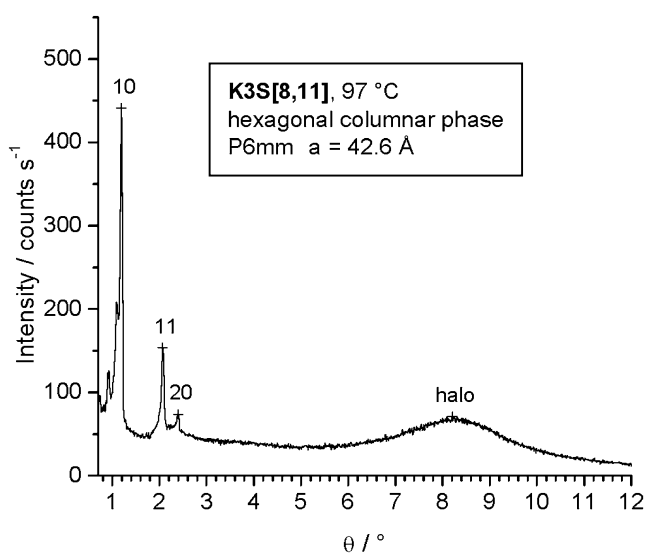r diagram representing temperature versus the number $n$ of C atoms in the perfluoroalkyl chains and the number $m$ in the alkyl chains clearly shows that, for the new compounds, the mesophase range is not affected dramatically by varying the alkyl or the perfluoroalkyl chain length, see figure 5. As usual, the transitions are shifted to higher temperatures with increasing $n$ [12, 16–18]. On the other hand, the appearance of the crystalline phase of **K3S[4,8]** [12] at room temperature with a mesophase range from $-11$ to $+41°C$ is somewhat surprising, as it does not fit the trends of the other compounds. The non-fluorinated analogues [19] do not show liquid crystallinity.

The spherulitic textures of the three-chain acids **K3S** revealed the presence of a columnar phase, see figure 6. Each single X-ray diffractogram of these compounds exhibits reflections with the distances $d_{hk0}$ in the ratio $1 : 1/\sqrt{3} : 1/2$, which corresponds to a hexagonal lattice. A typical example of an X-ray diffractogram is shown in figure 7; the results are summarized in table 2.

Using two different methods, we calculated the number $N$ of molecules per motif (lattice element), which is equal to the number of molecules per unit cell in a hexagonal columnar lattice. The first method (leading to $N_M$) uses the density $\rho$ (estimated to $1\,g\,cm^{-3}$ [14]) and the molecular mass $M$ of the compounds. The second method (leading to $N_{\Delta V}$) is based on the volume $V_{Mol}$ of one molecule, calculated by volume increments $\Delta V$ of different molecular parts. The final $N$ is the

Table 1. Transition temperatures *T* and enthalpies $\Delta H$ for the three-chain acids **K3S** (DSC, 2nd heating, $10\,\mathrm{K\,min^{-1}}$).

| *n,m* | Cr$_1$ | $T/°C$ ($\Delta H/\mathrm{kJ\,mol^{-1}}$) | Cr$_2$ | $T/°C$ ($\Delta H/\mathrm{kJ\,mol^{-1}}$) | Col | $T/°C$ ($\Delta H/\mathrm{kJ\,mol^{-1}}$) | I | Ref. |
|---|---|---|---|---|---|---|---|---|
| 6,8 | • | 34.5(10.9) | • | 53.0 (39.4) | • | 76.5 (2.6) | • | |
| 6,11 | • | 47.0 (20.2) | • | 58.0 (43.0) | • | 80.0 (3.0) | • | |
| 8,8 | • | 66.5 (−3.9) | • | 84.0 (55.3) | • | 103.0 (3.5) | • | |
| 8,11 | • | 80.5 (56.5) | • | 87.0 (5.4) | • | 105.0 (2.9) | • | |
| 10,8 | • | — | — | 98.5 (49.0) | • | **122.5 (3.8)** | • | |
| 10,11 | • | — | — | 106.5 (69.2) | • | 122.5 (3.1) | • | |
| 4,4 | • | — | — | 43 | • | [34][a] | • | [10] |
| 4,8 | • | — | — | −11 (12.2) | • | 41 (2.3) | • | [12] |
| 6,4 | • | 30 (2.1) | • | 51 (8.3) | • | 79 (2.3) | • | [10, 11][b] |
| 6,6 | • | 49 (19.7) | • | 76 (3.5) | • | 80 (3.6) | • | [12] |
| 8,4 | • | — | — | 100 (47.2) | • | 111 (5.0) | • | [12] |

[a]Monotropic phase
[b]Values were taken from [11].
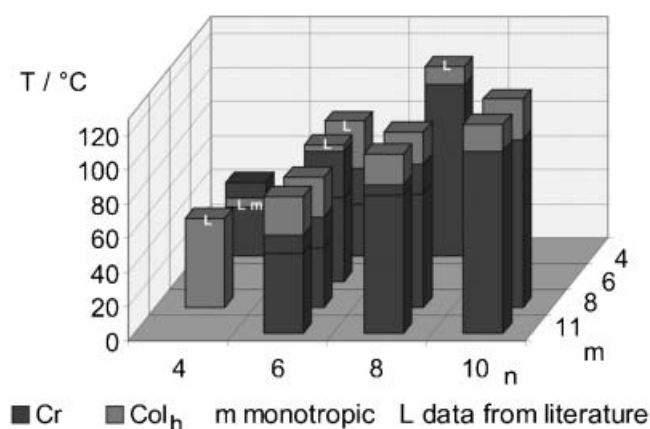


Figure 5. 3D bar diagram representing thermal behaviour of three-chain acids **K3S[n,m]** (cf. table 1). *n,m* are the lengths of the perfluoroalkyl and the alkyl chain, respectively.



Figure 7. Typical X-ray diffractogram of a Col$_h$ phase of **K3S**. The occurrence of the small 'peaks' left of the 10-reflection is explained in the text.

Table 2. X-ray data for the mesophases of the three-chain acids **K3S**. T=measurement temperaline; $\theta$=reflection angle with the indexation $hk$=10/11/20.

| *n,m* | $T/°C^{a}$ | Lattice parameter/Å | $\theta/°$ measured, *calculated*[b] |
|---|---|---|---|
| 10,11 | 125 | *a*=45.1 | 1.13/1.97/2.26 |
| | | halo: 5.5 | *1.13/1.96/2.26* |
| 10,8 | 110 | *a*=42.8 | 1.19/2.07/2.39 |
| | | halo: 5.5 | *1.19/2.06/2.38* |
| 8,11 | 97 | *a*=42.6 | 1.19/2.07/2.40 |
| | | halo: 5.4 | *1.20/2.08/2.40* |
| 8,8 | 50 | *a*=39.5 | 1.29/2.24/2.59 |
| | | halo: 5.4 | *1.29/2.24/2.58* |
| 6,11 | 70 | *a*=40.0 | 1.26/2.21/2.55 |
| | | halo: 5.2 | *1.27/2.21/2.55* |
| 6,8 | 65 | *a*=36.4 | 1.39/2.43/2.80 |
| | | halo: 5.2 | *1.40/2.43/2.80* |



Figure 6. Typical spherulitic texture of **K3S[8,11]** after slow cooling from the isotropic phase to 106°C.

Table 3. Number of molecules $N$ in the $Col_h$ phases of the three-chain acids **K3S**. For parameter definitions see text.

| $n,m$ | $a/Å$ | $M/g\,mol^{-1}$ | $N_M$ | $V_{Mol}/Å^3$ | $N_{\Delta V}$ | $N$ |
|---|---|---|---|---|---|---|
| 10,11 | 45.1 | 2186 | 1.9 | 1697 | 2.3 | 2 |
| 10,8 | 42.8 | 2060 | 1.9 | 1542 | 2.3 | 2 |
| 8,11 | 42.6 | 1886 | 2.0 | 1503 | 2.3 | 2 |
| 8,8 | 39.5 | 1760 | 1.8 | 1349 | 2.2 | 2 |
| 6,11 | 40.0 | 1586 | 2.1 | 1309 | 2.3 | 2 |
| 6,8 | 36.4 | 1460 | 1.9 | 1155 | 2.2 | 2 |



Figure 9. (*a*) Comparison of the X-ray diffractograms of **K3S[*n,m*]**, normalized to the 10-reflection. The arrows indicate the decrease in intensity of the 11-reflection with increasing *n*. (*b*) Ratio of the intensities of the 11- and 20-reflection.

average rounded value of these two numbers. The details of these calculations are described in a previous paper [14], and the results are summarized in table 3. In each case, two molecules can be found per motif. The resulting arrangement in such a hexagonal columnar phase is schematically shown in figure 8.

Up to this point, the results obtained for each three-chain acid confirm the $Col_h$ mesophase type shown by the literature compounds [11, 12]. However, the availability now of two homologous series of the three-chain acids **K3S[*n,m*]** with *m*=8 and 11 allowed an interesting comparison of all X-ray diffractograms of these compounds, as shown in figure 9 (*a*). There, the small angle diffractograms have been normalized to the 10-reflection. For both series, the intensity of the 20-reflection remains nearly constant, whereas the 11-reflection decreases strongly in intensity with increasing *n*, as indicated by arrows. We calculated the ratio $I_{11}/I_{20}$ of these reflections in order to quantify this tendency. The resulting six values are plotted in figure 9 (*b*).

In general, the 11-reflection is indicative of a hexagonal columnar mesophase. With increasing per-fluoroalkyl chain length *n*, i.e. with decreasing 11-intensity, the diffractograms seem to become more 'lamellar-like', but still keeping their hexagonal character, as indicated by the presence of the 11-reflection in all cases. So, the hexagonal columnar morphology of the three-chain acids seem to alter towards a lamellar structure, without totally achieving it. Several hypotheses may explain this decrease in intensity on elongation of the perfluoroalkyl chains: (1) step-by-step, the
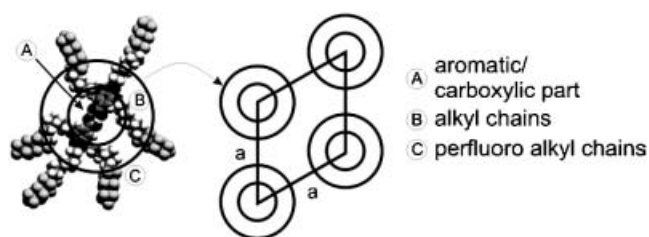


Figure 8. Schematic model of the dimer arrangement of **K3S** in a hexagonal columnar lattice.
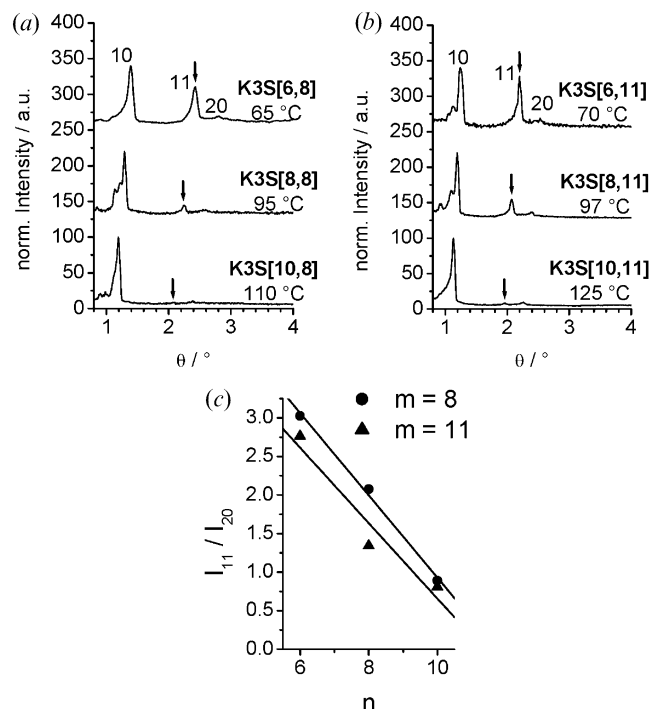
columns lose their hexagonal correlation towards a lamello–columnar phase [20]; (2) the molecular shape *remains unaffected* by increasing *n*, only the structure-factor changes in such a way that the $I_{11}/I_{20}$ ratio decreases; (3) the molecular shape *is affected* by an increasing *n* and causes a change in the morphology. Consequently, the structure factor will change. The first possibility seems not to be realistic. As the final result of the rearrangement, placing the columns into layers without any interlayer correlation would lead to a less dense packing, resulting also in a smaller 20-intensity. Additionally, during this rearrangement the inter-columnar distance should show a greater increase with respect to that of a pure hexagonal lattice. However, while the analogous two-chain acids **K2S** maintain their pure $Col_h$ phase with a lattice parameter *a*—which increases by about 3.7 Å from **K2S[8,8]** (*a*=42.6 Å) to **K2S[10,8]** (*a*=46.3 Å) [15]—the lattice parameter of the three-chain acids **K3S** in question increases only by 3.3 Å (see table 2), which is not a larger but a smaller increase.

We favour hypothesis (3), i.e. the molecular shape is affected by an increasing *n*, because it is well known [18, 21, 22] that perfluoroalkyl chains tend to arrange parallel, especially longer ones. In order to verify this with respect to hypothesis (2), we used several molecular

models, fitted them into the lattice, simulated the X-ray diffractograms, calculated the $I_{11}/I_{20}$ ratio and compared these results with the experimental data.

As two molecules have been found for one hexagonal unit cell (see table 3 and figure 8), our models are based on a carboxylic dimer. In the first model, all perfluoroalkyl and alkyl chains are radially arranged around the dimeric centre, leading to a circular-like arrangement of the dimers. Deviations from this ideal arrangement in
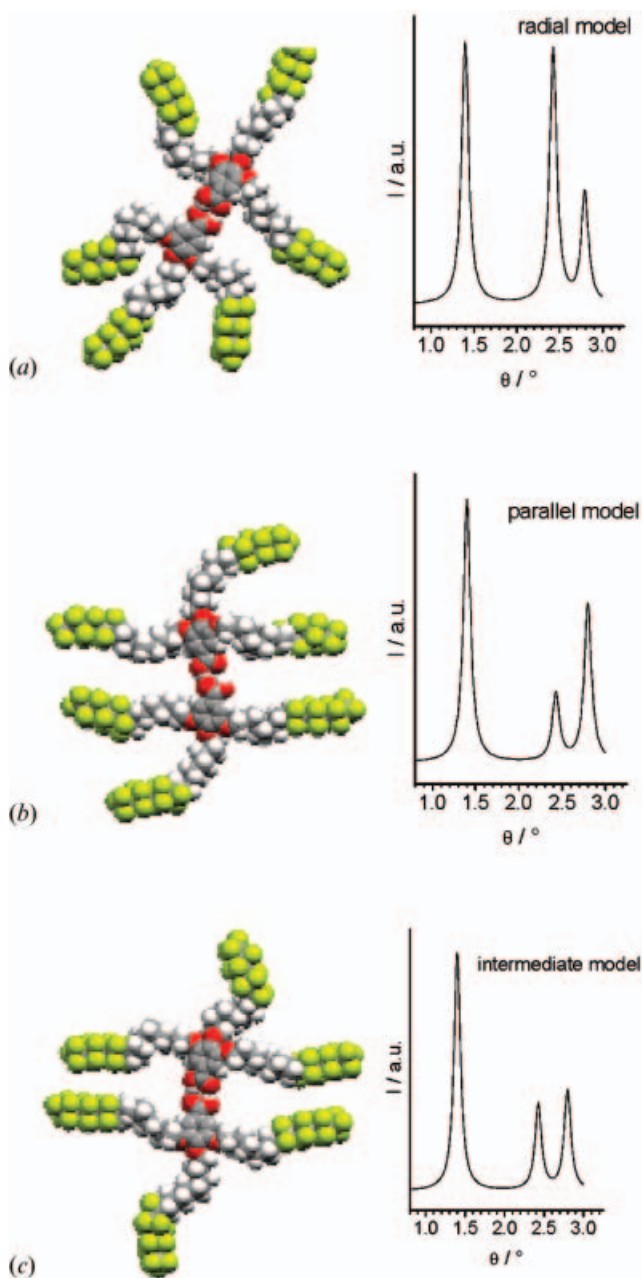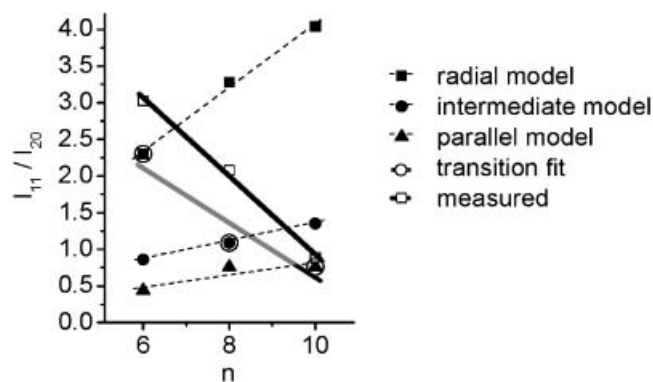


Figure 11. Dependence of the $I_{11}/I_{20}$ ratios of **K3S[n,8]** on their perfluoroalkyl chain length $n$, obtained from simulated X-ray diffractograms for the 'radial', 'parallel' and 'intermediate' models. Transition fit: simulated values for the transition from the 'radial' via the 'intermediate' to the 'parallel' model. Measured: measured transition values.

the plotted model are caused by the necessity of efficient space filling. This 'radial' model is shown in figure 10(a). In the second model, the alkyl chains maintain their radial arrangement; however, the perfluoroalkyl chains are packed parallel to each other, leading to the 'parallel' model, see figure 10(b). In the last model an intermediate situation is considered: four perfluoroalkyl chains are parallel, two maintaining their position from the radial model. Each of these three



Figure 10. Models of the three-chain acids **K3S[8,8]**: (a) 'radial' (b) 'parallel' (c) 'intermediate' model.
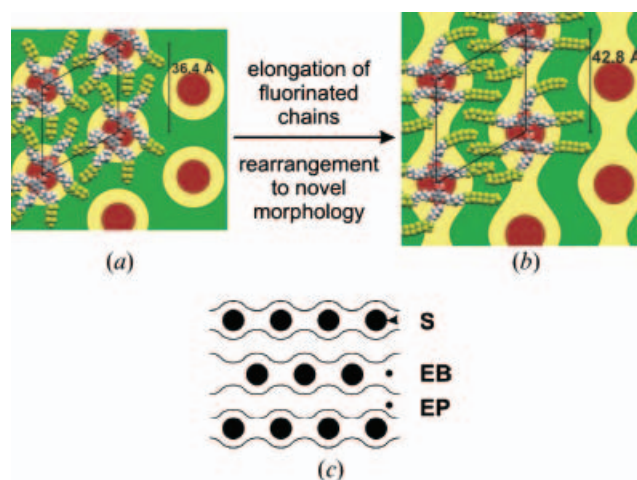


Figure 12. Schematic structure of the different morphologies of three-chain acids **K3S**. (a) Arrangement with core–shell columns on a hexagonal array, realized for short perfluoroalkyl chains ($n=6$). (b) Novel mesophase with a 'hexagonal columns-in-lamellae' ABC structure realized for long perfluoroalkyl chains ($n=10$). (c) 'Rectangular columns-in-lamellae' morphology of the linear ABC triblock copolymer poly(ethylene-*alt*-propylene)-*block*-poly(ethylene-*co*-butylene)-*block*-polystyrene (EPEBS) [23].

models has been realized with the alkyl chain length $m=8$ and the perfluoroalkyl chain length $n=6,8,10$.

For the simulation, we placed each dimer in its hexagonal columnar unit cell. The lattice parameters were taken from the X-ray measurements (see table 2). The simulation of the X-ray diffractograms of the three models yielded the first three reflections of a hexagonal pattern (10-, 11- and 20-reflection, see figure 10). In order to compare the simulated diffractograms with the measured ones, we calculated the simulated $I_{11}/I_{20}$ ratios. For each model ('radial', 'parallel', 'intermediate'), the resulting values are plotted against the number $n$ of $CF_2$ groups (see figure 11).

Obviously, none of the three models (all with increasing $I_{11}/I_{20}$ ratios versus increasing $n$) can explain the measured *decrease* in the $I_{11}/I_{20}$ ratio, shown in figure 9. In consequence, hypothesis (2) is unlikely to be an explanation for the observed behaviour. We therefore considered hypothesis (3) with a change of the molecular shape from one to the other model with increasing $n$. For the smallest member ($n=6$) of the homologous series of **K3S[n,8]**, we start with the 'radial' model, see figures 8 and 10(*a*), because of its intensive hexagonal columnar 11-reflection. For the largest member ($n=10$), i.e. with a tendency of parallel packing of the long perfluoroalkyl chains, we assumed the 'parallel' model. For the acid with a medium perfluoroalkyl chain length ($n=8$), we let the pure 'radial' model change to the pure 'parallel' model. Therefore, we used the 'intermediate' model, see figure 10(*c*). The simulated $I_{11}/I_{20}$ ratio now fits very well into a *decreasing* dependency of the $I_{11}/I_{20}$ ratio for the homologous series **K3S[n,8]** with $n=6,8,10$, shown in figure 11. The similarity to the measured values, with respect at least to the decreasing tendency, is quite reasonable, see figure 9(*b*).

In consequence, we can establish a new liquid crystalline morphology. The members of the series **K3S[n,m]** ($m=8,11$) with the shortest perfluoroalkyl chain ($n=6$) exhibit hexagonally arranged, core–shell columns within the matrix of perfluoroalkyl chains ('radial' model). This situation is shown in figure 12(*a*). After an intermediate situation for $n=8$ (in approximation the 'intermediate' model), the longest perfluoroalkyl chains in **K3S[n,m]** with $n=10$ are packed parallel to each other. Consequently, they cannot fill the matrix around the columns, but form an undulated layer between them, which still remains in a hexagonal lattice, as shown in figure 12(*b*).

This new morphology is the first established liquid crystalline phase of an ABC mesogen with no anisometric unit in the basic molecule. To a certain degree, it seems to be comparable to the morphology of a linear ABC triblock copolymer, realized with the block copolymer poly(ethylene-*alt*-propylene)-*block*-poly(ethylene-*co*-butylene)-*block*-polystyrene EPEBS [23]. Here the S-block, polystyrene, forms columns on a rectangular lattice, surrounded by the undulated EB-block, poly-(ethylene-*co*-butylene). The EP-block, poly(ethylene-*alt*-propylene), also forms an undulated lamella between the other blocks, see figure 12(*c*). Due to this similarity, we like to denominate the described new LC mesophase as a 'hexagonal columns-in-lamellae' morphology. A similar morphology has been assumed by Tschierske *et al.* [24], but no analytical proof was given.

## 3. Conclusion

One- and two-chain acids **K1S[n,m]** and **K2S[n,m]** have been reported to exhibit smectic and columnar phases, respectively [15]. Due to a third perfluoroalkylalkyloxy chain in the three-chain acids **K3S[n,m]**, which should increase the wedge-shape character of the molecules, we expected first a mesophase with an even higher interface curvature, resulting in, for example, a spheroidic cubic phase. However, textures and X-ray diffractograms showed only the presence of hexagonal columnar phases instead.

For the compounds with increasing perfluoroalkyl chain length $n$, a closer comparative examination of the small angle diffractograms revealed a rearrangement from a classical $Col_h$ phase to a novel mesophase. In the $Col_h$ phase (realized for **K3S[6,m]**) the perfluorohexyl chains form a *matrix* around core–shell columns, whereas in the new mesophase (**K3S[10,m]**) the parallel aligned perfluorodecyl groups segregate into their own undulated *layer* between the hexagonally arranged core–shell columns. The result is a novel 'hexagonal columns-in-lamellae' morphology of low molar mass ABC-mesogens.

In principle, the analogy to morphologies of linear ABC triblock copolymers reveals the pronounced similarities of both low molar mass and polymeric segregated systems. Because of the large number of exciting new morphologies known for numerous linear ABC triblock copolymers, one could expect that with this new 'hexagonal columns-in-lamellae' morphology the door to many other morphologies of linear ABC-mesogens may have been opened.

For another class of block copolymers, i.e. star-like ABC triblock copolymers, this opening has already been realized. The combination of aggregating and segregating parts, together with a third conventional anisometric (calamitic) unit in one molecule, proved to favour the formation of a sequence of classical and new phases, as shown in figure 13(*a*) [25]. However in this
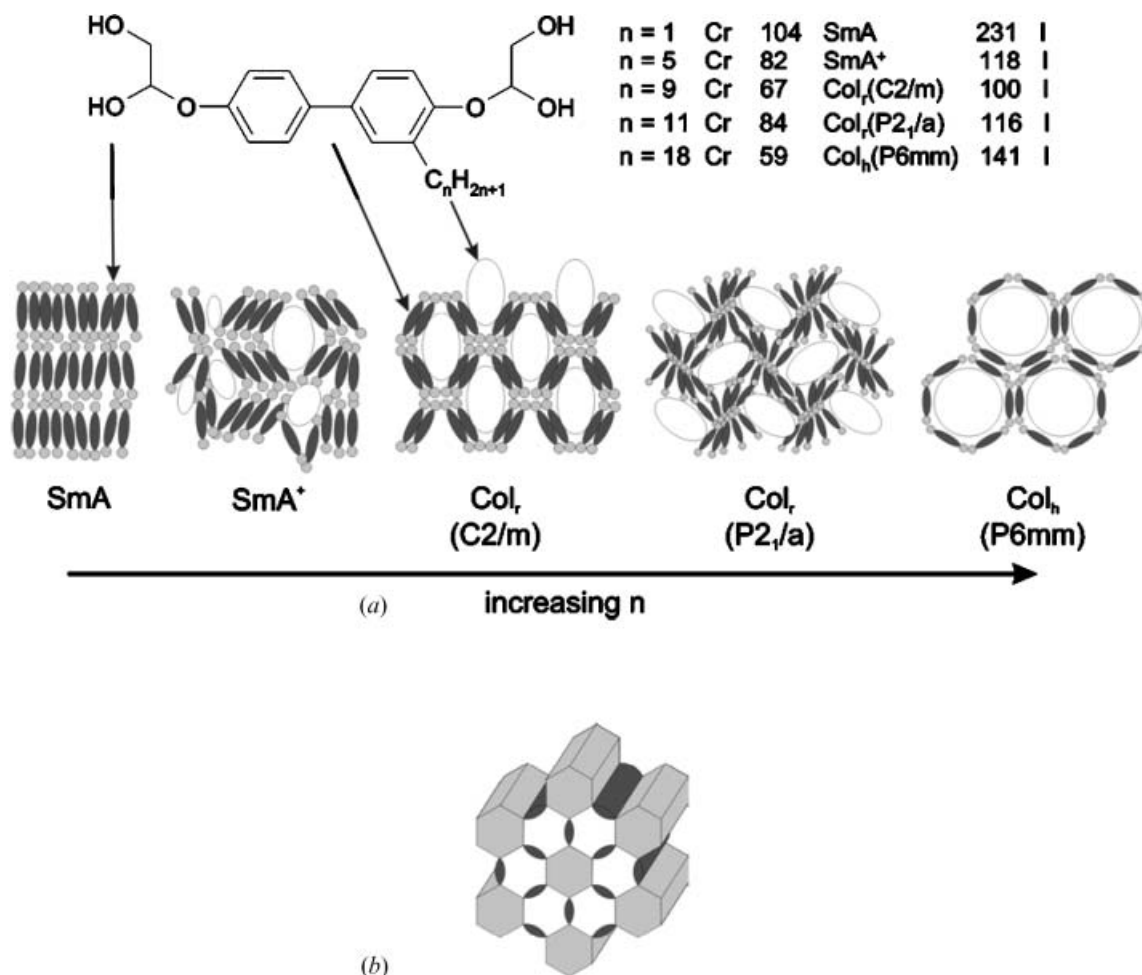
Figure 13.   (*a*) Liquid crystalline phases of a bolaamphiphile [25]; (*b*) possible morphology of a star-like ABC triblock copolymer [26].

case, the driving force for the generation of a new phase seems to be mainly the anisometry of the calamitic part. Some of these morphologies resemble those of star-like ABC copolymers, illustrated in figure 13 (*b*) [26] as an example of the given Col$_h$ phase.

### 4.   Experimental methods

The synthesis and chemical characterization of the three-chain acids **K3S[*n,m*]** was described earlier in detail [14]. Polarizing optical microscopy was performed on a Nikon Diaphot 300 with hot stage Mettler FP82. Photographs were taken with a Nikon F4 camera. Thermal analysis was performed with a Perkin-Elmer DSC 7 apparatus at a heating rate of $10 \, K \, min^{-1}$.

X-ray diffractograms were recorded on a Guinier diffractometer device from Huber, Germany, with a scintillation counter. The standard resolution was $0.01°$ with 20 s data collection per step. The X-ray tube contained a copper anode with a quartz crystal as monochromator (Cu K$\alpha_1$-radiation, $\lambda = 1.54051 \, Å$) from

Seifert, Germany. The samples were prepared in glass capillaries of 1 mm diameter. The reflection-like peaks beneath the real, indexed peaks can be explained by the use of a slit-diaphragm in front of the detector together with the presence of a non-statistical distribution of the domains. The molecular models as well as the X-ray simulation were obtained with the program 'Cerius 2' from msi.

### References

[1] I.W. Hamley, *The Physics of Block Copolymers*. Oxford University Press, Oxford (1998); L. Leibler. *Macromolecules*, **13**, 1602 (1980).

[2] C. Tschierske. *J. mater. Chem.*, **8**, 1485 (1998).

[3] K. Borisch, S. Diele, P. Göring, H. Müller, C. Tschierske, *Liq. Cryst.*, **22**, 427 (1997); K. Borisch, S. Diele, P. Göring, C. Tschierske. *Chem. Commun.*, 237 (1996).

[4] Y. Mogi, H. Kotsuji, Y. Kaneko, K. Mori, Y. Matsushita, I. Noda, *Macromolecules*, **25**, 5408 (1992); Y. Mogi, K. Mori, Y. Matsushita, I. Noda. *Macromolecules*, **25**, 5412 (1992).

[5] R. Stadler, C. Auschra, J. Beckmann, U. Krappe, I. Voigt-Martin, L. Leibler. *Macromolecules*, **28**, 3080 (1995).

[6] H. Hückstädt, A. Göpfert, V. Abetz, *Polymer*, **41**, 9089 (2000); H. Ott, V. Abetz and V. Altstädt. *Macromolecules*, **34**, 2121 (2001).

[7] U. Breiner, U. Krappe, V. Abetz, R. Stadler, *Macromol. Chem. Phys.*, **198**, 1051 (1997); U. Breiner, U. Krappe, T. Jakob, V. Abetz, R. Stadler. *Polym. Bull.*, **40**, 219 (1998).

[8] U. Breiner, U. Krappe, R. Stadler, *Macromol. rapid Commun.*, **17**, 567 (1996); T. Goldacker, V. Abetz. *Macromol. rapid Commun.*, **20**, 415 (1999).

[9] F. Guittard, S. Geribaldi, *J. fluorine Chem.*, **107**, 363 (2001); F. Guittard, E. Taffin de Givenchy, S. Geribaldi, A. Cambon. *J. fluorine Chem.*, **100**, 85 (1999); R. Miethchen, M. Hein. *Carbohydr. Res.*, **327**, 169 (2000); V. Percec, D. Schlueter, G. Ungar. *Macromolecules*, **30**, 645 (1997).

[10] X. Cheng, M.K. Das, S. Diele, C. Tschierske. *Langmuir*, **18**, 6521 (2002).

[11] V. Percec, C. Schluter, Y.K. Kwon, J. Blackwell, M. Möller, P.J. Slangen. *Macromolecules*, **28**, 8807 (1995).

[12] G. Johansson, V. Percec, G. Ungar, J.P. Zhou. *Macromolecules*, **29**, 646 (1996).

[13] V. Percec, G. Johansson, G. Ungar, J. Zhou. *J. Am. chem. Soc.*, **118**, 9855 (1996).

[14] A. Eisenmann, E. Valaitytė, G. Lattermann. *Liq. Cryst.* (submitted) (2003).

[15] A. Eisenmann, E. Valaitytė, G. Lattermann. *Liq. Cryst.* (submitted) (2003).

[16] H.T. Nguyen, G. Sigaud, M.F. Achard, F. Hardouin, R.J. Twieg, K. Betterton. *Liq. Cryst.*, **10**, 389 (1991).

[17] Y.H. Chiang, A.E. Ames, R.A. Gaudiana, T.G. Adams. *Mol. Cryst. liq. Cryst.*, **208**, 85 (1991).

[18] R. Twieg, K. Betterton, R. DiPietro, D. Gravert, C. Nguyen, H.T. Nguyen, A. Babeau, C. Destrade, G. Sigaud. *Mol. Cryst. liq. Cryst.*, **217**, 201 (1992).

[19] V. Percec, J. Heck. *Polym. Bull.*, **25**, 431 (1991).

[20] G. Lattermann, S. Schmidt, R. Kleppinger, J.H. Wendorff. *Adv. Mater.*, **4**, 30 (1992).

[21] G. Pelzl, S. Diele, D. Lose, B.I. Ostrovski, W. Weissflog, *Cryst. Res. Technol.*, **32**, 99 (1997); D. Lose, S. Diele, G. Pelzl, E. Dietzmann, W. Weissflog. *Liq. Cryst.*, **24**, 707 (1998).

[22] J. Gao, S.A. Rice. *J. chem. Phys.*, **99**, 7020 (1993).

[23] C. Neumann, D.R. Loveday, V. Abetz, R. Stadler. *Macromolecules*, **31**, 2493 (1998).

[24] R. Plehnert, J.A. Schröter, C. Tschierske. *J. mater. Chem.*, **8**, 2611 (1998).

[25] M. Kölbel, T. Beyersdorff, X.H. Cheng, C. Tschierske. *J. Am. chem. Soc.*, **123**, 6809 (2001).

[26] H. Hückstädt, A. Göpfert, V. Abetz. *Macromol. Chem. Phys.*, **201**, 296 (2000).